Muon $g-2$ experiments

Alberto Lusiani
Scuola Normale Superiore and INFN, sezione di Pisa

Selected puzzles in particle physics
20-22 December 2016, Laboratori Nazionali di Frascati

Introduction

Definition

$\vec{\mu}_\mu = g_\mu (-1) \frac{e}{2mc} \vec{S}_\mu$ ($\vec{\mu}_\mu$ muon magnetic moment, $\vec{S}$ = spin)

muon anomaly $a_\mu = \frac{g-2}{2}$

Muon $g-2$ Standard Model test

$(a_\mu^{\text{exp}} - a_\mu^{\text{th}}) \pm \delta(a_\mu^{\text{exp}} - a_\mu^{\text{th}}) = (270 \pm 76) \cdot 10^{-11}$ corresponds to 3.6σ discrepancy

- experiment and theory error $\delta(a_\mu^{\text{exp}} - a_\mu^{\text{th}}) = \delta a_\mu^{\text{exp}} \oplus \delta a_\mu^{\text{th}}$
  - $\delta a_\mu^{\text{exp}} = 0.54\,\text{ppm}$ WA $\simeq$ BNL E821 final report 2006
  - $\delta a_\mu^{\text{th}} = 0.36\,\text{ppm}$ DHMZ 2016 preliminary, Tau 2016
    - $$\begin{aligned} \delta a_\mu^{\text{SM}} &= \delta a_\mu^{\text{QED}} \oplus \delta a_\mu^{\text{EW}} \oplus \delta a_\mu^{\text{hadLBL}} \oplus \delta a_\mu^{\text{hadLO}} \oplus \delta a_\mu^{\text{hadNLO}} \oplus \delta a_\mu^{\text{hadNNLO}} \\ &= (\,0.04 \oplus 1 \oplus 26 \oplus 33 \oplus 0.9 \oplus 0.1\,) \cdot 10^{-11} \\ &= (\quad \oplus \quad \oplus 0.22\,\text{ppm} \oplus 0.28\,\text{ppm} \oplus \quad \oplus \quad) \end{aligned}$$

      DHMZ 2016 preliminary, Tau 2016
  - experimental measurements determine/dominate $\delta a_\mu^{\text{exp}}$ and $\delta a_\mu^{\text{hadLO}}$
    - also $\delta a_\mu^{\text{hadNLO}}$ and $\delta a_\mu^{\text{hadNNLO}}$
    - in the future probably also $\delta a_\mu^{\text{hadLBL}}$


a_μ^{exp}

Muon $g-2$ experimental measurements

Authors	Year/Lab	a_μ	δa_μ
Garwin *et al.*	'60 CERN	0.001 13(14)	124 ppt
Charpak *et al.*	'61 CERN	0.001 145(22)	19 ppt
Charpak *et al.*	'62 CERN	0.001 162(5)	4.3 ppt
Farley *et al.*	'66 CERN	0.001 165(3)	2.7 ppt
Bailey *et al.*	'68 CERN	0.001 166 16(31)	270 ppm
Bailey *et al.*	'79 CERN	0.001 165 923 0(84)	8 ppm
Brown *et al.*	'00 BNL μ^+	0.001 165 919 1(59)	
Brown *et al.*	'01 BNL μ^+	0.001 165 920 2(14)(6)	
Bennett *et al.*	'02 BNL μ^+	0.001 165 920 4(7)(5)	
Bennett *et al.*	'04 BNL μ^-	0.001 165 921 4(8)(3)	
BNL E821 & CODATA 2010	'06 BNL	0.001 165 920 91(63)	0.54 ppm
WA (CODATA 2008)		0.001 165 920 89(63)	0.54 ppm

Muon $g-2$ measurement method

- measure muon spin precession in magnetic field
- since 3rd CERN experiment, muons accumulated at "magic" energy in a storage ring

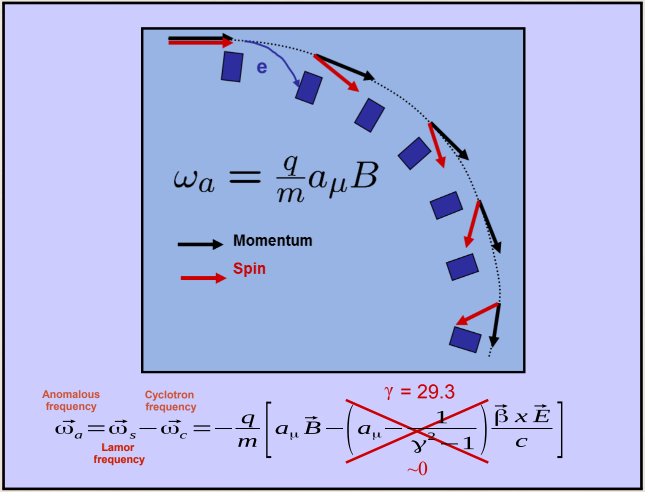

Muon $g-2$ measurement method

- $\vec{\omega}_s = -\frac{gq\vec{B}}{2m} - (1-\gamma)\frac{q\vec{B}}{\gamma m}$
- $\vec{\omega}_c = -\frac{q\vec{B}}{\gamma m}$
- $\vec{\omega}_a \equiv \vec{\omega}_s - \vec{\omega}_c = -\left(\frac{g-2}{2}\right)\frac{q\vec{B}}{m} = -a_\mu \frac{q\vec{B}}{m}$
- average B in muon orbit measured with proton spin precession frequency $\tilde{\omega}_p$

$a_\mu^{\rm exp}$ determination

$$a_\mu^{\rm exp} = \frac{g_e}{2}\frac{\omega_a}{\tilde{\omega}_p}\frac{m_\mu}{m_e}\frac{\mu_p}{\mu_e}$$

- $\omega_a/\tilde{\omega}_p$ (540 ppb) from muon $g-2$ exp WA
- g_e (0.0003 ppb) from a_e measurements
- m_μ/m_e (22 ppb) from CODATA 2014
- μ_p/μ_e (3 ppb) from CODATA 2014

Relevant muon $g-2$ $(\omega_a/\tilde{\omega}_p)$ experiments

- BNL E821, E_{magic}, final report in 2008
- FNAL E989, E_{magic}, beginning data-taking in 2017, goal $\delta a_\mu^{\mathrm{exp}} = 0.14\,\mathrm{ppm}$
- J-PARC E34, ultra-cold muons, Sep 2016 revised TDR goal $\delta a_\mu^{\mathrm{exp}} = 0.37\,\mathrm{ppm}$

in the following

- present BNL E821 methods and uncertainties
  - BNL E821 dominates $\omega_a/\tilde{\omega}_p$ WA
- describe differences in FNAL E989 and J-PARC E34
- status update on experimental inputs for a_μ^{hadLO}

Muon $g-2$ SM test uncertainties summary

Quantity	Uncertainty $\times 10^{-11}$	$\delta a_\mu / a_\mu$ (ppb)
ω_a statistical	53	458
ω_a systematic	24	210
$\tilde{\omega}_p$ systematic	20	170
CODATA m_μ / m_e	2.6	22
CODATA μ_p / μ_e	0.35	3
Electron g factor, g_e	0.000035	0.0003
QED	0.08	0.7
EW	1	8.6
hadLBL	26	223
hadLO	33	280
hadNLO	0.9	7.6
hadNNLO	0.1	0.86

ω_a measurement method

- inject polarized muons (from forward pion decay) into storage ring
- let them decay
- along the ring, count number of electrons above some threshold energy over time
  $N_e(E_e > E_{thr}) = N_0(E_{thr}) e^{-t/\gamma\tau} [1 + A(E_{thr}) \cos(\omega_a t + \phi(E_{thr}))]$

asymmetry and ω_a dependence come from muon decay & Lorentz boost

- decay electron angle and energy distribution depend on angle between $\vec{p}_e$ and $\vec{s}_\mu$

  $dP(y,\theta) \propto n(y)[1 + A(y) cos\theta]\, dy\, d\Omega$ (in approximation $m_\mu >> m_e$)

  $y = p_e / p_{e\ max}$, $cos\theta = \widehat{p_e} \cdot \widehat{s_\mu}$
- while muons decay, angle between $\vec{p}_\mu$ and $\vec{s}_\mu$ rotates with ω_a, changing boost
- with large muon momentum in LAB
  - electron momentum direction is about aligned with muon momentum
  - electron momentum size depends on angle between $\vec{p}_e$ and $\vec{p}_\mu$ in muon rest frame

ω_a measurement method, E821 details

- p on target $\to$ pions, $\pi \to \mu\nu$, high momentum muons 97% polarized
- inject polarized muons in 14 m diameter storage ring
- $B = 1.45\,\text{T}$, muons at magic energy with $\gamma = 29.3$
- vertical beam focusing with electric field quadrupoles
- detect electrons with EM calorimeter modules along interior of storage ring

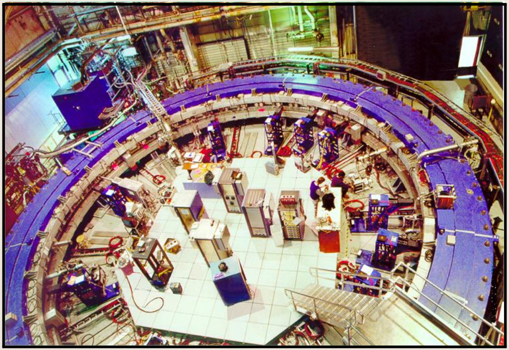

ω_a measurement statistical uncertainty

- fit $N_e(E_e > E_{\text{thr}}) = N_0(E_{\text{thr}})e^{-t/\gamma\tau}[1 + A(E_{\text{thr}})\cos(\omega_a t + \phi(E_{\text{thr}}))]$
- $\dfrac{\delta\omega_a}{\omega_a} = \dfrac{1}{\omega_a \gamma \tau_\mu}\sqrt{\dfrac{2}{NA^2P^2}}$ N = number of muons, P = muon polarization, A = asymmetry
  - improves with B field since $\omega_a \propto B$
  - improves with number of muons, asymmetry, polarization
  - improves with muon momentum (γ)

E_{thr} dependence for E821

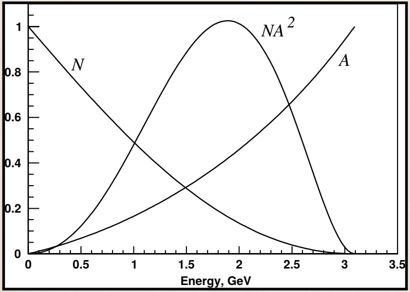

E_{thr} dependence including E821 acceptance

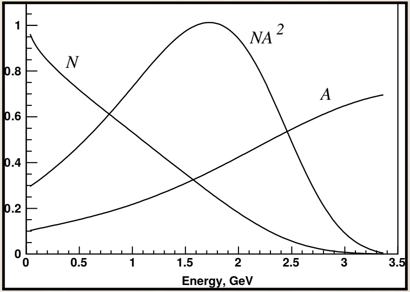

ω_a measurement method, E821 wiggle plot

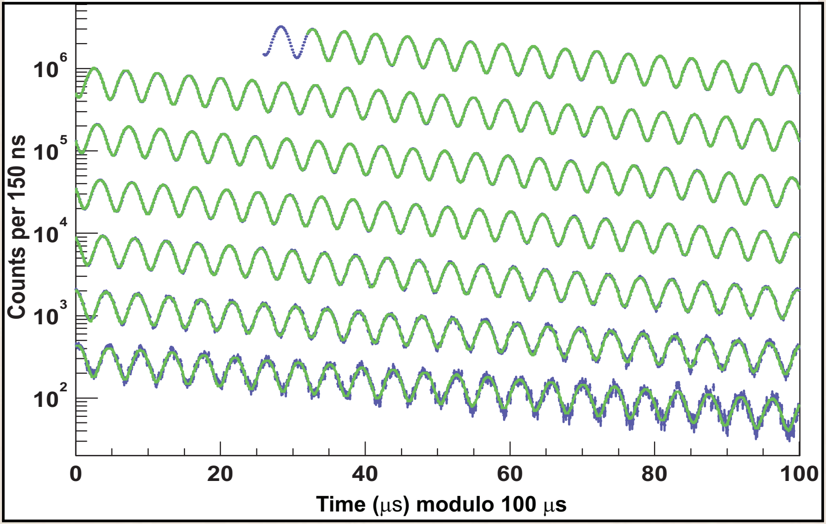

ω_a measurement systematic uncertainties (E821)

	E821 [ppb]
detector gain variation	120
event pileup	80
lost muons	90
coherent betatron oscillations	70
electric-field and pitch corrections	50

ω_a systematics from detector gain variation (E821)

- detector gain variation causes effective E_{thr} variation $\Rightarrow \omega_a$ shift
- large event rate variation over one fill causes deterministic gain variation within fills
- laser gain calibration system could not be used (unknown systematics)
- fit gain variation in fill from E spectrum end-point: $\dfrac{G(t) - G(\infty)}{G(\infty)} = f \cdot \dfrac{\bar{E}(t) - \bar{E}(\infty)}{\bar{E}(\infty)}$
- estimated systematic is 100% of the correction

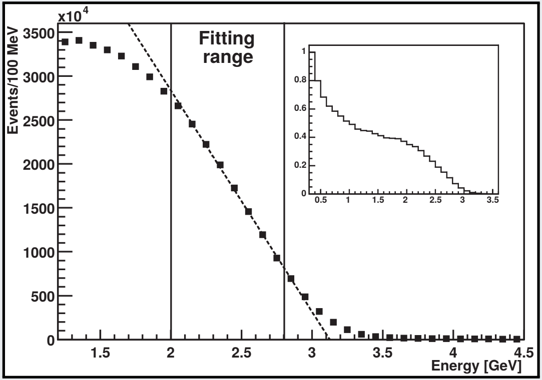

ω_a systematics from event pileup (E821)

- double event pileup probability $\propto$ event rate square ($e^{2t/\gamma\tau}$), affects ω_a fit
- at each time, contribution from pileup to energy distribution subtracted on average
- $D(E, t)$ energy distribution of actually pileup of "trigger" pulse and "shadow" pulse
- $S_T(E, t)$ energy distribution of "trigger" pulse
- $S_S(E, t)$ energy distribution of additional "shadow" pulse on top of "trigger" pulse
- pileup contribution $P(E, t) = D(E, t) - S_T(E, t) - S_S(E, t)$
- subtracting $P(E, t)$ from measured energy distribution restores true energy distribution
  - consistency check: resulting energy distribution invariant w.r.t. event rate
  - use to correct above-energy-threshold counts
  - systematic uncertainty from approximations of procedure

ω_a systematics from event pileup (E821)

pileup contribution to N(E,t), $P(E,t) = D(E,t) - S_T(E,t) - S_S(E,t)$

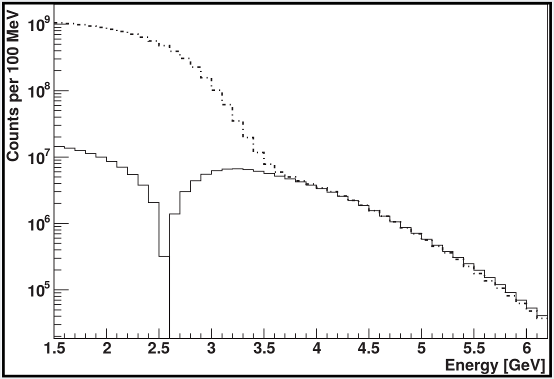

- dotted line corresponds to observed distribution
- pileup contribution is negative for $E < 2.5\,\text{GeV}$, but plotted as positive
- above $3.1\,\text{GeV}$ total observed distribution corresponds to pileup as expected

ω_a systematics from lost muons (E821)

- storage ring defects may originate periodic forces that lead to muon losses
- beam scraping short after injection reduces further losses of marginal injected muons
- dedicated scintillators on triple coincidence detect lost muons
- muon loss is included in the fit
- uncertainties on lost muons phase contribute to ω_a systematic uncertainty

ω_a systematics, fast rotation interlude (E821)

- muons are injected as a short bunch
- muon momentum spread progressively distributes bunch over whole ring
- bunch spreading measured from event rate variation with cyclotron frequency

detected electron rate modulation with cyclotron frequency, decreasing in amplitude as the bunch spreads

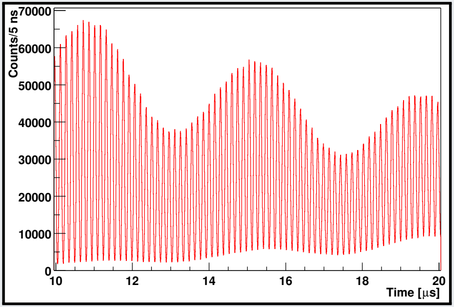

reconstructed muons radial distribution from fast rotation measurement

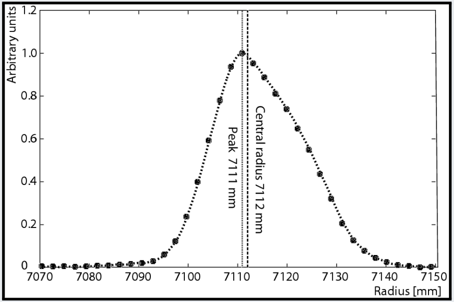

ω_a systematics from coherent betatron oscillations or CBO (E821)

- electric field quadrupole focusing causes betatron oscillations
- beam oscillations detected with scintillating fiber beam monitors
- beam oscillations start with amplitude determined by beam injection
- beam oscillations amplitude decays due to tune spread (focusing quads imperfections)

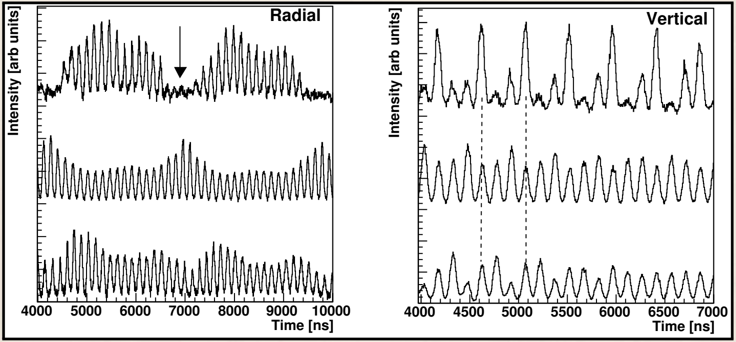

muons on inner, middle, outer fiber

muons on top, middle bottom fiber

ω_a systematics from coherent betatron oscillations or CBO (E821)

Physical frequency	Variable	Expression	Frequency	Period
Anomalous precession	f_a	$\frac{e}{2\pi m} a_\mu B$	0.23 MHz	4.37 μs
Cyclotron	f_c	$\frac{v}{2\pi R_0}$	6.71 MHz	149 ns
Horizontal betatron	f_x	$\sqrt{1-n} f_c$	6.23 MHz	160 ns
Vertical betatron	f_y	$\sqrt{n} f_c$	2.48 MHz	402 ns
Horizontal CBO	f_{CBO}	$f_c - f_x$	0.48 MHz	2.10 μs
Vertical waist	f_{VW}	$f_c - 2f_y$	1.74 MHz	0.57 μs

- horizontal CBO modulates detector acceptance hence N, A and ϕ
- amplitude and decay time of all modulations are fit on wiggle plot
- CBO effects suppressed by factor $\sim$10 by approx. detector azymuthal symmetry
- CBO systematic contribution from varying remaining fixed parameters not fit on data

ω_a systematics from electric field and pitch corrections (E821)

electric-field correction

- momentum and beam radial spread induces non-zero electric field corrections
- $\left\langle \frac{\delta\omega_a}{\omega_a} \right\rangle = -2\beta^2 n(1-n) \left\langle \left(\frac{R}{R_0} \right)^2 \right\rangle$
- radial spread measured from fast rotation analysis
- additionally
  - σ on muon radius vs. E quadrupole center ± 0.5 mm (± 0.01 ppm in a_μ)
  - σ on muon vertical position vs. E quadrupole center ± 1 mm (± 0.02 ppm in a_μ)
- typical uncertainty on correction 50 ppb for single run

pitch correction

- vertical inclination of muon momentum of angle ψ, $\frac{\delta\omega_a}{\omega_a} = -\frac{1}{2}\psi^2$
- ψ_m = amplitude of angle oscillation
- $\langle \psi_m^2 \rangle = n\langle y^2 \rangle / R_0^2$, $\quad \langle y^2 \rangle$ mean-squared vertical spread measured with FBM
- average effect of oscillation on muon ensemble $\frac{1}{4}\langle \psi_m^2 \rangle$
- typical uncertainty on correction 40 ppb for single run

$\tilde{\omega}_p$ measurement systematic uncertainties (E821)

B field accurately measured with NMR probes

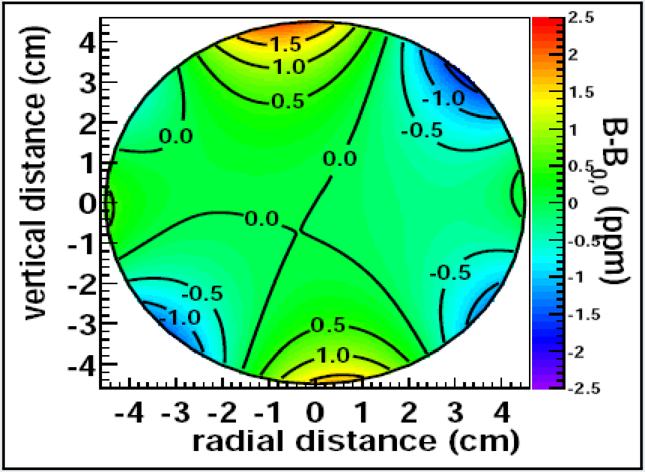

$\tilde{\omega}_p$ measurement systematic uncertainties (E821)

	E821 [ppm]
Absolute calibration of standard probe	0.05
Calibration of trolley probes	0.09
Trolley measurements of B_0	0.05
Interpolation with fixed probes	0.07
Uncertainty from muon distribution	0.03
Others †	0.10
Total systematic error on ω_p	0.17

† Higher multipoles, trolley temperature and its power supply voltage response, and eddy currents from the kicker

$\tilde{\omega}_p$ systematics from absolute calibration of standard probe (E821)

- ideal case: precession of free protons in vacuum, unperturbed B field
- reality:
  - protons in water with a $CuSO_4$ additive
  - B field perturbed by magnetization of the materials in probe and trolley

absolute calibration

- absolute calibration probe, protons in water sphere, low magnetic susceptibility
- correction of $\tilde{\omega}_p$ in water to vacuum using
  - ratio of g for proton in water to g of e in ground state of hydrogen atom (10 ppb)
  - ratio of g electron to proton in hydrogen (9 ppb)
  - proton g corrections from vacuum to bound state (theory calculatiom, 9 ppb)

$\tilde{\omega}_p$ systematics from calibration of trolley probes (E821)

- all probes were calibrated with the standard probe
- measure same place B with different probes $\Rightarrow$ spread of relative calibration (20 ppb)
- temperature and power supply voltages effects studied (50 ppb)
- absolute calibration at athmospheric pressure but probes used in vacuum
- effect of diamagnetic O_2 estimated by replacing air with N_2, 37 ppb correction

$\tilde{\omega}_p$ systematics from trolley measurements of B_0 (E821)

- NMR probes measure $|\vec{B}|$
  - measure B_x in some locations
  - estimate that approximation $B_y = |\vec{B}|$ is OK to 10 ppb

FNAL E989 experiment

E821 magnet trip from BNL to FNAL

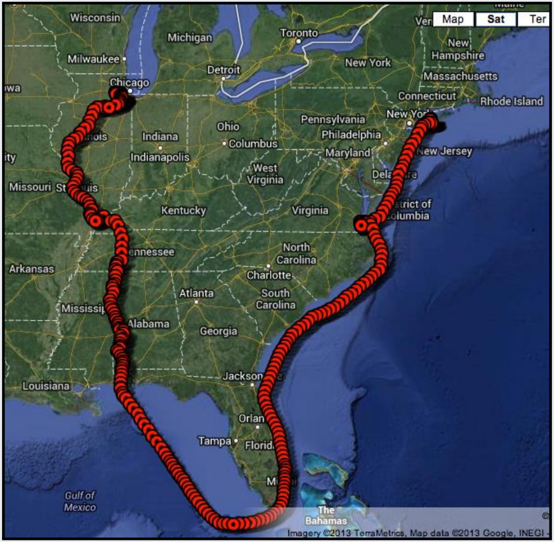

FNAL E989 experiment

Reduce statistical $\delta\omega_a$ from 458 ppb to 100 ppb

- just need 21 times more muons, $1.5 \cdot 10^{11}$

Item	Estimate
Protons per fill on target	10^{12} p
Positive-charged secondaries with $dp/p = \pm 2\%$	4.8×10^7
π^+ fraction of secondaries	0.48
π^+ flux entering FODO decay line	$> 2 \times 10^7$
Pion decay to muons in 220 m of M2/M3 line	0.72
Muon capture fraction with $dp/p < \pm 0.5\%$	0.0036
Muon survive decay 1800 m to storage ring	0.90
Muons flux at inflector entrance (per fill)	4.7×10^4
Transmission and storage using $(dp/p)_\mu = \pm 0.5\%$	0.10 ± 0.04
Stored muons per fill	$(4.7 \pm 1.9) \times 10^3$
Positrons accepted per fill (factors 0.15 x 0.63)	444 ± 180
Number of fills for 1.8 $\times 10^{11}$ events	$(4.1 \pm 1.7) \times 10^8$ fills
Time to collect statistics	(13 ± 5) months
Beam-on commissioning	2 months
Dedicated systematic studies periods	2 months
Net running time required	17 ± 5 months

Chris Polly, FNAL E989, FNAL, August 2016

First challenge…getting the statistics

Muon g-2

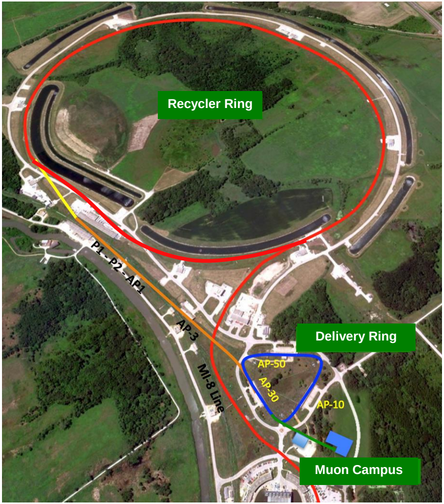

Achieving required statistics is a primary concern

- Need a factor 21 more statistics than BNL
- Beam power reduced by 4

Need a factor of 85 improvement in integrated beam coming from many other factors

- Collection of pions from lens
- Capture of decay muons in FODO channel
- p_π closer to magic momentum
- Longer decay channel
- Increased injection efficiency
- Earlier start time of fits
- Longer runtime

Chris Polly, Fermi Summer Students, 2 August 2016 43

Chris Polly, FNAL E989, FNAL, August 2016

Detectors

Muon g-2

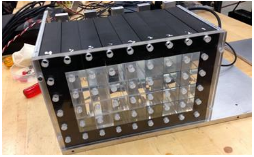

- Calorimeters 24 6x9 PbF2 crystal arrays with SiPM readout
- New electronics and DAQ
- Three 1500 channel straw trackers to precisely monitor properties of stored muon beam via tracking of Michel decay positrons
- Auxiliary detectors and slow controls to monitor beam properties and environmental conditions

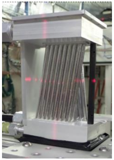

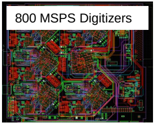

Top view of 1 of 12 vacuum chambers

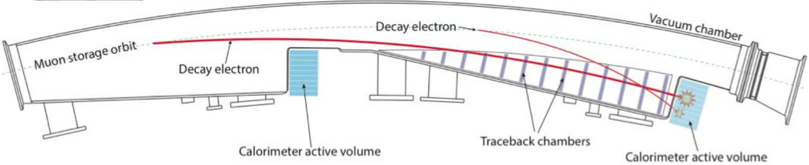

Chris Polly, Fermi Summer Students, 2 August 2016 44

Chris Polly, FNAL E989, FNAL, August 2016

Second challenge..controlling ω_a systematic

Muon g-2

Category	E821 [ppb]	E989 Improvement Plans	Goal [ppb]
Gain changes	120	Better laser calibration	
		low-energy threshold	20
Pileup	80	Low-energy samples recorded	
		calorimeter segmentation	40
Lost muons	90	Better collimation in ring	20
CBO	70	Higher n value (frequency)	
		Better match of beamline to ring	< 30
E and pitch	50	Improved tracker	
		Precise storage ring simulations	30
Total	180	Quadrature sum	70

- Tackling each of the major systematic errors with knowledge gained from BNL E821

David Hertzog, FNAL E989, FCCP 2016

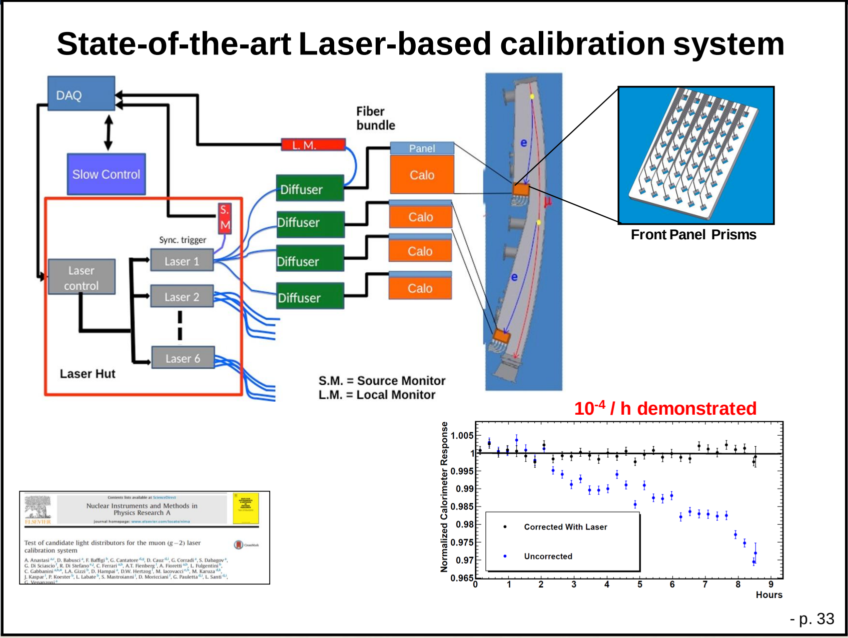

FNAL E989 experiment

Reduce systematic $\delta\tilde{\omega}_p$ from 170 ppb to 70 ppb

Category	E821 [ppb]	Main E989 Improvement Plans	Goal [ppb]
Absolute field calibration	50	Improved T stability and monitoring, precision tests in MRI solenoid with thermal enclosure, new improved calibration probes	35
Trolley probe calibrations	90	3-axis motion of plunging probe, higher accuracy position determination by physical stops/optical methods, more frequent calibration, smaller field gradients, smaller abs cal probe to calibrate all trolley probes	30
Trolley measurements of B_0	50	Reduced/measured rail irregularities; reduced position uncertainty by factor of 2; stabilized magnet field during measurements; smaller field gradients	30
Fixed probe interpolation	70	Better temp. stability of the magnet, more frequent trolley runs, more fixed probes	30
Muon distribution	30	Improved field uniformity, improved muon tracking	10
External fields	–	Measure external fields; active feedback	5
Others †	100	Improved trolley power supply; calibrate and reduce temperature effects on trolley; measure kicker field transients, measure/reduce O_2 and image effects	30
Total syst. unc. on ω_p	170		70

Chris Polly, FNAL E989, FNAL, August 2016

Field stability and uniformity improvements

Muon g-2

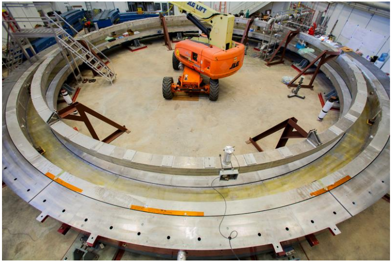

- Environmental
  - 2'9" heavily-reinforced floor installed on 12' deep excavation of undisturbed soil
  - Temperature control to +/- 1C
- Construction tolerances
  - 26 ton pieces of yoke steel (30 of them) placed to 125 micron tolerance
  - Pole pieces aligned to 25 micron
- 9 months of interactively shimming B-field with bits of steel and current loops

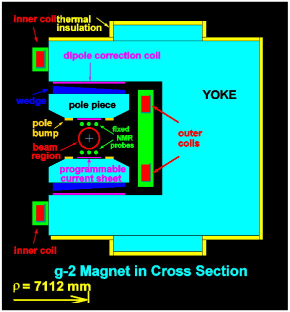

Chris Polly, Fermi Summer Students, 2 August 2016 47

Chris Polly, FNAL E989, FNAL, August 2016

Monitoring magnetic field

Muon g-2

- Fixed probes track field at top/bottom of vacuum chamber monitor field 24/7
  - Only half of 400 were used in BNL (primarily due to being in gradients that were too large) → building better NMR probes and in some case adjusting positions
- NMR trolley pulls out of garage every day or two and maps field where muons live
  - More frequent trolley runs (every 2-3 days) to reduce extrapolation error
  - Optical encoders for better position resolution
- Digitizing FID signals

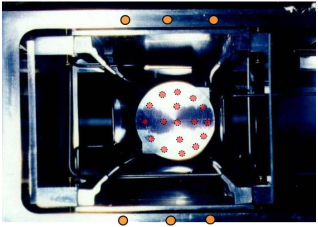

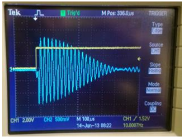

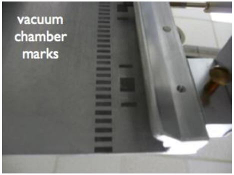

Chris Polly, Fermi Summer Students, 2 August 2016 48

FNAL E989 experiment

Shimming successfully completed in August 2016

- 10 months of align and optimize our shim knobs:
  - 72 pole pieces
  - 800 wedge shims
  - 9000 iron shim foils
  - ...

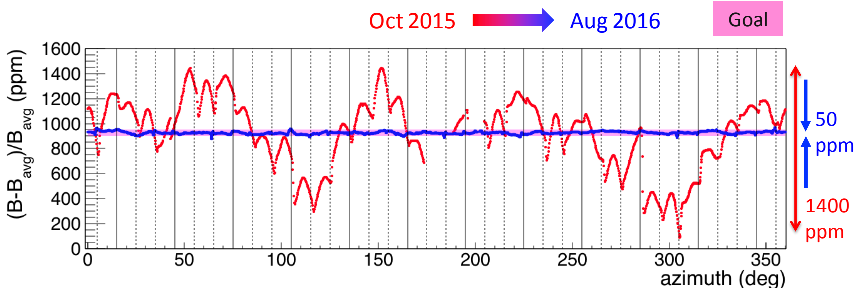

Shimming goal achieved with $\Delta B < \pm 25$ ppm ✓

Chris Polly, FNAL E989, FNAL, August 2016

Absolute calibration

Muon g-2

- Setting up a dedicated test facility at ANL to study and develop improved absolute calibration tests
- Learning how to make better spheres… water diamagnetic shielding is 26 ppm
- Developing He3 magnetometry

Absolute calibration probe with spherical water sample

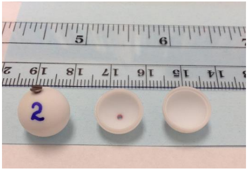

Chris Polly, FNAL E989, FNAL, August 2016

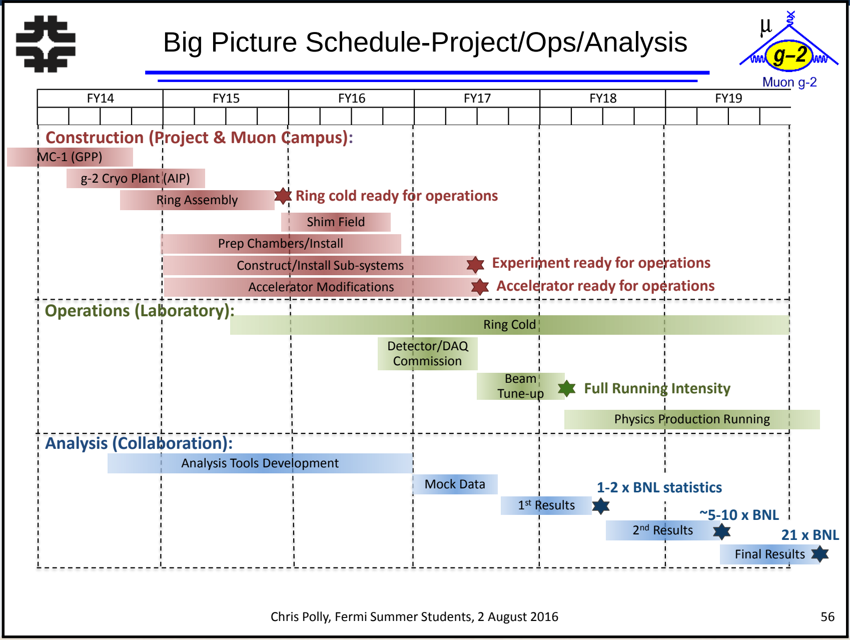

J-PARC E34 experiment

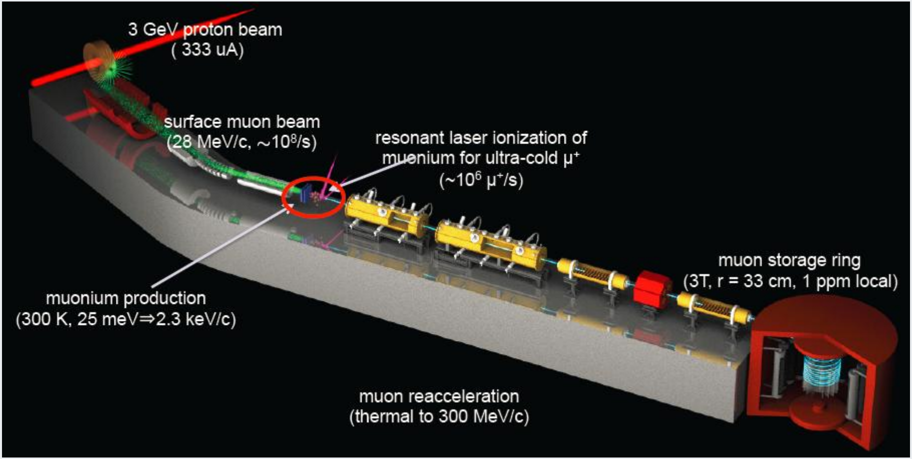

Michael Eads, J-PARC E34, FPCP 2015

Motivation

- Different (and very complementary) approach to Fermilab experiment
- If you start with muons with ~zero transverse momentum, you don't need any electric fields

$$\vec{\omega_a} = \frac{e}{mc}\left[a\vec{B} - \left(a - \frac{1}{\gamma^2 - 1}\right)\vec{\beta} \times \vec{E}\right]$$

- Experiment can then be much more compact

Michael Eads, J-PARC E34, FPCP 2015

Motivation

- Different (and very complementary) approach to Fermilab experiment
- If you start with muons with ~zero transverse momentum, you don't need any electric fields

$$\vec{\omega_a} = \frac{e}{mc}\left[a\vec{B} - \left(a - \frac{1}{\gamma^2 - 1}\right)\vec{\beta} \times \vec{E}\right]$$

- Experiment can then be much more compact

Michael Eads, J-PARC E34, FPCP 2015

Ultra-cold Muons

- Protons on graphite target produce polarized surface muons
- Muons stopped to form Muonium atoms, drift into vacuum
- Ionized with two lasers, accelerated with LINAC
- Produces beam of 300 MeV ultra-cold muons with 50% polarization

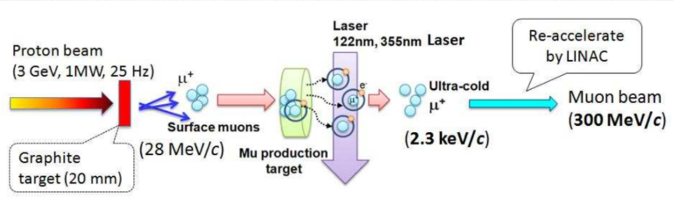

M. Eads
FPCP, Nagoya
29 May 2015

Michael Eads, J-PARC E34, FPCP 2015

Muonium Production

- Limiting factor is diffusion of Muonium from room temperature source
- Recent successes at TRIUMF with silica aerogel with laser-ablated micro-channels
- Currently predicting total muon rate into g-2 detector of 0.2 x 10^6/s

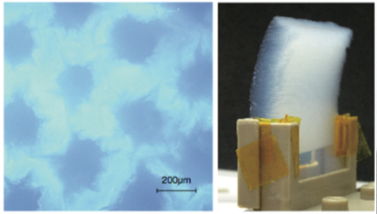

Prog. Theor. Exp. Phys. (2013)
arXiv: 1407.8248

M. Eads
FPCP, Nagoya
29 May 2015

Michael Eads, J-PARC E34, FPCP 2015

Injection to Storage Ring

- 300 MeV muons injected into 3.0T, 33cm-radius solenoidal magnet
- Magnetic coils give kick to stabilize vertically
- Very weak magnetic focusing

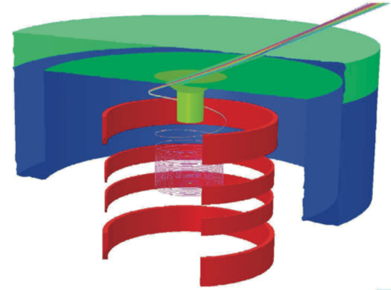

M. Eads
FPCP, Nagoya
29 May 2015

Michael Eads, J-PARC E34, FPCP 2015

Detectors

- Double-sided silicon sensors inside of orbit, 200 µm pitch
- ~40 vanes, each 6cm in radius, 12cm in height
- Total of 98 planes, 691k strips
- E/B fields from detectors under study

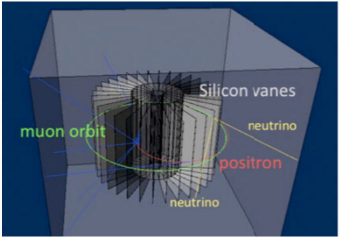

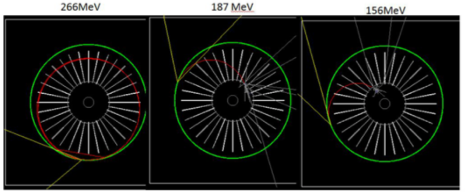

Figure 6: Example positron trajectories in the detector system at three different energies of positrons. The green circle is the muon beam orbit. The red trajectory is the trace of the positron track. The white tracks are photons.

M. Eads
FPCP, Nagoya
29 May 2015

29

Tsutomu Mibe, J-PARC E34, November 2016

Comparison of experiments

	BNL E821	J-PARC E34
muon momentum	3.09 GeV/c	0.3 GeV/c
storage ring radius	7 m	0.33 m
storage field	1.5 T	3.0 T
focusing field (n-index)	0.14 (electric)	1.5 E-4 (magnetic)
average field uniformity	≈1 ppm	<< 1ppm
(local uniformity)	≈50 ppm	≈1ppm
Injection	inflector + kick	spiral + kick
Injection efficiency	3-5%	80%
muon spin reversal	--	pulse-to-pulse
positron measurement	calorimeters	tracking
positron acceptance*	65%	≈100%
muon polarization	≈100%	≈50%
events to 0.46 ppm	9×10^9	5×10^{11}

* in the energy region of interest

30

J-PARC E34 experiment systematics

?

Tsutomu Mibe, J-PARC E34, November 2016

TDR

Technical Design Report
for
the Measurement of the Muon Anomalous
Magnetic Moment $g-2$ and Electric
Dipole Moment at J-PARC

May 15, 2015

prepared by 144 authors

Summary

In summary, this experiment intends to reach statistical uncertainties for muon $g-2$ of 0.37 ppm and for muon EDM of $1.3 \times 10^{-21} e \cdot \mathrm{cm}$, during an acquisition time of 2×10^7 seconds of high-quality data, with a completely new experimental technique based on an ultra-cold muon beam and a compact storage ring. We will show in this document that our current understanding of the available beam power, the efficiency of the ultra-cold muon source, the muon acceleration, injection, and storage, and decay detection, all indicate that this is achievable. The statistical reach in the quoted running time is lower than we originally proposed. However, the $g-2$ sensitivity, even at this level, should exceed that of BNL E821 and provide an independent test of the three to four sigma discrepancy with the Standard Model prediction. Moreover, it would reduce the existing upper limit for the muon EDM by a factor of about 70. In the process of achieving these important goals, we would also be able to identify and understand any systematic uncertainties that may have to be reduced before attaining the final goal as originally proposed. In parallel, we will continue R&D, especially on the ultra-cold muon source intensity, to further improve the sensitivity to the final goal of 0.1 ppm for $g-2$.

- TDR describes a technical design to achieve measurement of muon g-2 and EDM beyond BNL E821 precision.

	BNL E821		J-PARC E34
g-2:	0.46 ppm	→	0.37 ppm (→0.1ppm)
EDM:	0.9×10^{-19} ecm	→	1.3×10^{-21} ecm

33


a_μ^{hadLO}

$\sigma(e^+e^- \to \text{hadrons})$ measurements for a_μ^{hadLO}

- $e^+e^- \to$ hadrons   scanning CM energy
- $e^+e^- \to \gamma_{\text{ISR}}$hadrons   fixed CM energy, varying E_γ

Achim Denig, Precision hadronic physics

Precision measurements of σ_{had} via ISR

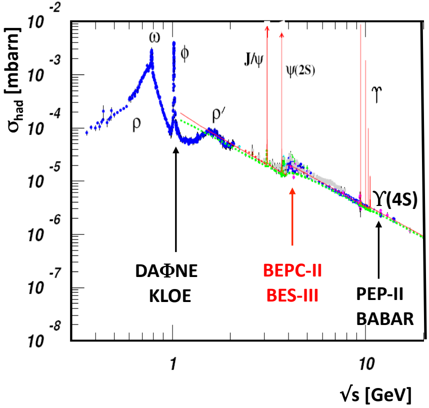

Approach for measuring hadronic cross section at modern particle factories with fixed c.m.s. energy √s:

Initial State Radiation (ISR)

Radiator function $H(M_{hadr})$ describes probability for ISR emission

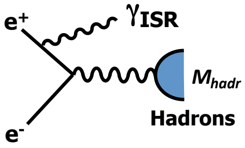

ISR method allows to access mass range $M_{hadr} < \sqrt{s}$

P1: Precision Hadron Physics: $(g-2)_\mu$ and $\alpha_{em}(M_Z^2)$

$\sigma(e^+e^- \to$ hadrons) measurements for a_μ^{hadLO} presented at Tau 2016

- **Experimental Measurements**
  - Pion form factor measurement and ISR at BESIII (Yaqian Wang)
  - QCD and R value measurement at BESIII [in progress] (Haiming HU)
  - New ISR results on $\sigma(\pi^+\pi^-\pi^0\pi^0)$ and $\pi^+\pi^-\eta$ from BaBar (K. Griessinger)
  - New ISR results on $\sigma(K_S K_L \pi^0, KSKL2pi0)$ from BaBar (Wolfgang Gradl)
  - Recent $e^+e^- \to$ hadrons results from SND at VEPP-2000 (Mikhail Achasov)
  - New $e^+e^- \to$ hadrons results from CMD-3 [in progress] (Simon Eidelman)
  - R measurement between 1.8 and 3.7 GeVat KEDR (Simon Eidelman)
  - New $e^+e^- \to$ hadrons results from Belle (Chengping Shen)
- **Muon $g-2$ hadronic contributions with Lattice**
  - Lattice calculation for LO hadr. contrib. to $(g-2)_\mu$ (Bipasha Chakraborty)
  - Lattice calculation for light-by-light hadr. contrib. to $(g-2)_\mu$ (Taku Izubuchi)

Progress on the experimental measurements of $e^+e^- \to$ hadrons

BESIII measurement $e^+e^- \to \pi^+\pi^-(\gamma)$ from 0.6 to 0.9 GeV

- use ISR technique
- 0.9% systematic precision (comparable to KLOE, *BABAR*)
- reached design luminosity $1 \cdot 10^{33}\,\text{cm}^{-2}\text{s}^{-1}$ at 3.773 GeV
- integrated BESIII corresponding muon $g-2$ contribution agrees more with KLOE than *BABAR* **but** there is a complex pattern of differences in the energy dependence
- adding BESIII measurement, muon anomaly discrepancy is confirmed
- planning measurements closer to threshold region
- planning measurements at high energies without requiring ISR photon detection
- under study $e^+e^- \to \pi^+\pi^-\pi^0(\pi^0)$

BESIII measurement on $e^+e^- \to$ hadrons in 2.0—4.6 GeV

- collected all planned data sets for QCD and R scan between 2.0-4.6 GeV
- analysis on 2.2324—3.671 GeVcompleted, prelim. result in review in BESIII
- in progress analysis for 3.85—4.6 GeV
- luminosity of 149 points measured with about 1% precision
- final overall measurement precision goal: 2.5—3.0%

Pion form factor measurement and ISR at BESIII (Yaqian Wang)

$\pi^+\pi^-$ Cross section comparison

Cross section

$$\sigma^{\rm bare}_{\pi\pi(\gamma_{\rm FSR})} = \frac{N_{\pi\pi\gamma}\cdot(1+\delta^{\pi\pi}_{\rm FSR})}{\mathcal{L}\cdot\epsilon^{\pi\pi\gamma}_{\rm global}\cdot H(s)\cdot\delta_{\rm vac}} \qquad \sigma^{\rm bare}_{\pi\pi(\gamma_{\rm FSR})} = \frac{N_{\pi\pi\gamma}}{N_{\mu\mu\gamma}}\cdot\frac{\epsilon^{\mu\mu\gamma}_{\rm global}}{\epsilon^{\pi\pi\gamma}_{\rm global}}\cdot\frac{1+\delta^{\mu\mu}_{\rm FSR}}{1+\delta^{\pi\pi}_{\rm FSR}}\cdot\sigma^{\rm bare}_{\mu\mu}$$

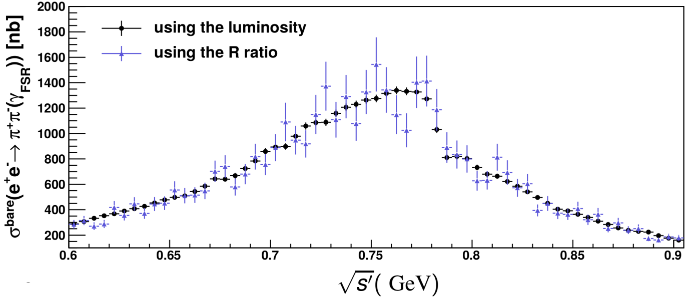

Relative difference: $(0.85 \pm 1.68)\%$

Good agreement!

Pion form factor measurement and ISR at BESIII (Yaqian Wang)

Contribution to $a_\mu^{\text{VP,LO}}$

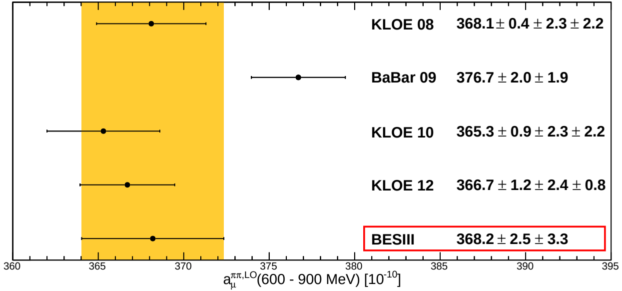

- Precision competitive with previous measurements
- BESIII measurement well agrees with KLOE
- Confirmed deviation between experiment and theory

Pion form factor measurement and ISR at BESIII (Yaqian Wang)

$\pi^+\pi^-$ Cross section comparison

Comparison with BaBar and KLOE

systematic shift

Agreement

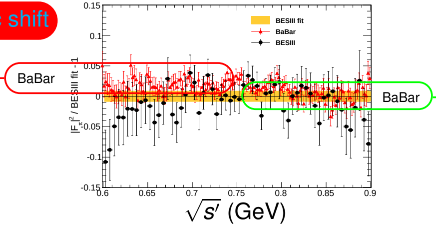

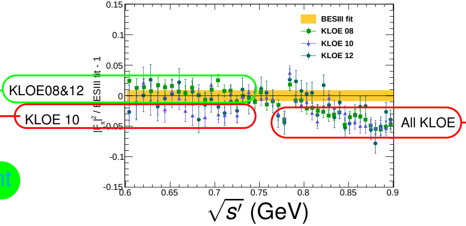

Agreement

systematic shift

Yaqian WANG (JGU) Pion Form Factor TAU 2016 23 / 25

Progress on the experimental measurements of $e^+e^- \to$ hadrons

BaBar ISR-technique measurements $e^+e^- \to$ hadrons (Griessinger+Gradl)

- $\pi^+\pi^-\pi^0\pi^0$, new, preliminary, 3.2% precision on a_μ contribution
- $\pi^+\pi^-\eta$, new, preliminary, 5.3% precision on a_μ contribution
- $K_S K_L \pi^0$, $K_S K_L 2\pi^0$, preliminary, $\sim$18% precision
  - all $KK\pi$ and $KK\pi\pi$ processes now measured by *BaBar*

New ISR results on $\sigma(\pi^+\pi^-\pi^0\pi^0)$ and $\pi^+\pi^-\eta$ from BaBar (K. Griessinger)

Contribution of $\pi^+\pi^-2\pi^0$ to $g_\mu - 2$

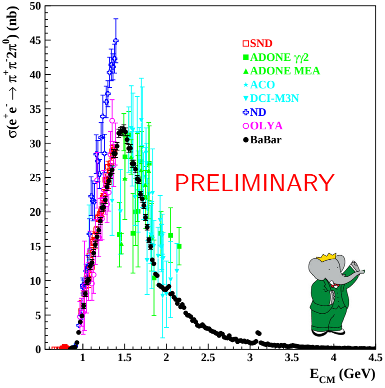

$$a_\mu^{\text{had}} = \frac{1}{4\pi^3}\int_{m_{\pi^0}^2}^{\infty} \frac{\sqrt{1-\frac{4m_e^2}{s}}}{1+\frac{2m_e^2}{s}} K_\mu(s)\sigma(s)\mathrm{d}s$$

New result starting at lower limit

$a_\mu(0.85 < \sqrt{s} < 1.8\,\text{GeV}) =$
$(17.9 \pm 0.1_{\text{stat}} \pm 0.6_{\text{syst}}) \times 10^{-10}$

New result in a wider energy range

$a_\mu(0.85 < \sqrt{s} < 3.0\,\text{GeV}) =$
$(21.8 \pm 0.1_{\text{stat}} \pm 0.7_{\text{syst}}) \times 10^{-10}$

New ISR results on $\sigma(\pi^+\pi^-\pi^0\pi^0)$ and $\pi^+\pi^-\eta$ from BaBar (K. Griessinger)

Cross section $e^+e^- \to \pi^+\pi^-\eta$

Contribution of $\pi^+\pi^-\eta$ to $g_\mu - 2$

$$a_\mu^{\rm had} = \frac{1}{4\pi^3}\int_{m^2_{\pi^0}}^{\infty} \frac{\sqrt{1-\frac{4m_e^2}{s}}}{1+\frac{2m_e^2}{s}} K_\mu(s)\sigma(s){\rm d}s$$

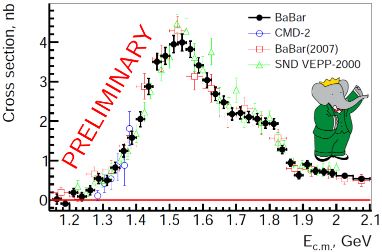

HLMNT 2011 [8]

$a_\mu(\sqrt{s} < 1.8\,\text{GeV}) = (0.88 \pm 0.10) \times 10^{-10}$

DHMZ 2011 [5]

$a_\mu(\sqrt{s} < 1.8\,\text{GeV}) = (1.15 \pm 0.06_{\rm stat} \pm 0.08_{\rm syst}) \times 10^{-10}$

New result

$a_\mu(\sqrt{s} < 1.8\,\text{GeV}) = (1.19 \pm 0.02_{\rm stat} \pm 0.06_{\rm syst}) \times 10^{-10}$

New ISR results on $\sigma(K_S K_L \pi^0, K_S K_L 2\pi^0)$ from BaBar (Wolfgang Gradl)

$K_S^0 K_L^0 \pi^0$ cross section

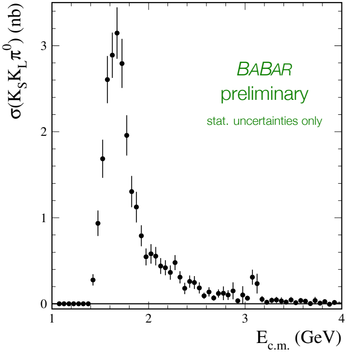

Systematic uncertainties include

- Background subtraction:
  $\approx 10\%$ for $M(K_S^0 K_L^0 \pi^0) < 2.2$ GeV, increasing to ≈ 80-100% above 3.2 GeV
- Efficiency corrections
  overall data-MC difference of $(-9.5 \pm 1.6)\%$

New ISR results on $\sigma(K_S K_L \pi^0, K_S K_L 2\pi^0)$ from BaBar (Wolfgang Gradl)

$K^0_S K^0_L \pi^0 \pi^0$ cross section

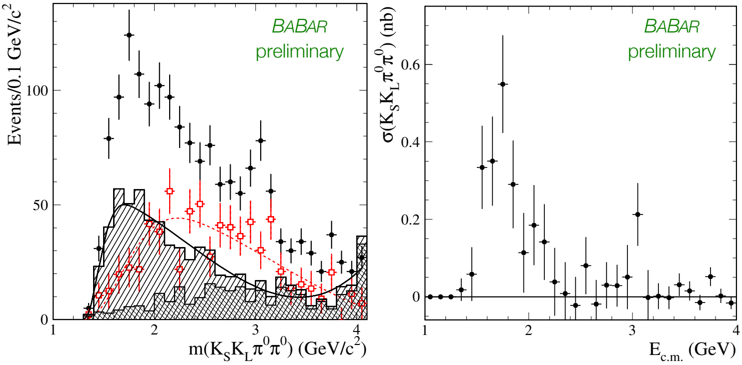

New ISR results on $\sigma(K_S K_L \pi^0, K_S K_L 2\pi^0)$ from BaBar (Wolfgang Gradl)

Summary

- Measure cross sections for $e^+e^- \to K^0_S K^0_L \pi^0(\pi^0)$
- Resonant substructure explored with $\mathcal{O}(10^2)$ events
- Contribution to a_μ:

$$a_\mu^{KK\pi\pi}(E_{\text{CM}} < 2\,\text{GeV}) \times 10^{10} = 3.31 \pm 0.58 \qquad \text{HLMNT 2011}$$

$$a_\mu^{\text{all}KK\pi\pi}(E_{\text{CM}} < 2\,\text{GeV}) \times 10^{10} = 2.41 \pm 0.11$$

- All $KK\pi$ and $KK\pi\pi$ now directly measured by *BABAR*
  no isospin relations needed any more for cross sections and dispersion relation!

- Branching fractions for J/ψ and ψ' to $K^0_S K^0_L \pi^0(\pi^0)$
  improved precision, first measurements

- Final word from *BABAR* for these channels.
  More progress: BESIII, Belle II, VEPP-2000

New ISR results on $\sigma(K_S K_L \pi^0, K_S K_L 2\pi^0)$ from BaBar (Wolfgang Gradl)

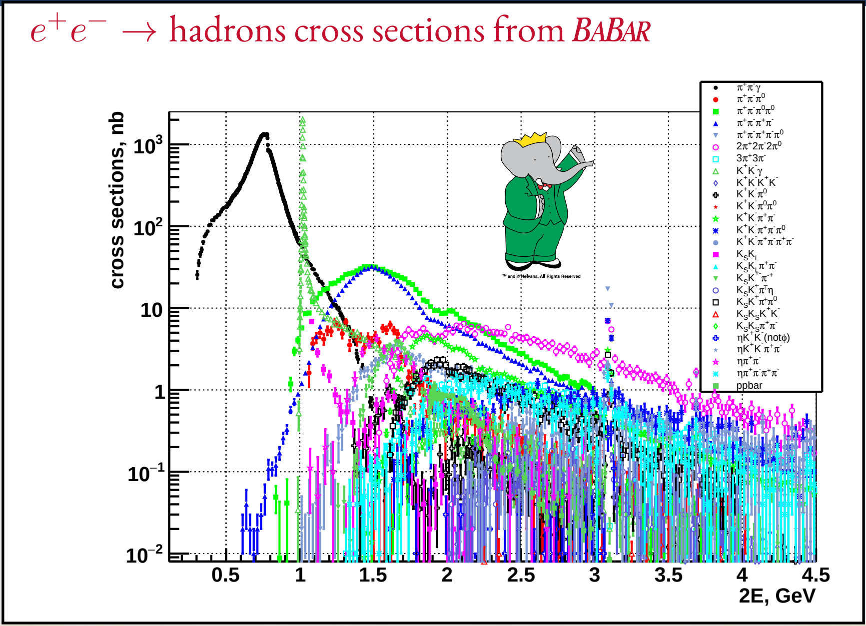

Progress on the experimental measurements of $e^+e^- \to$ hadrons

Novosibirsk, VEPP-2000 facility, 2010-2013, $L = 10^{32}\,\text{cm}^{-2}\text{s}^{-1}$, 60pb^{-1}

- completed upgrade to get $10\times$ luminosity
- since 2012, beam energies measured with Compton backscattering of laser

Novosibirsk, SND at VEPP-2000 measurements

- updated precision measurements
  - $e^+e^- \to \pi^0\gamma$, systematic precision 1.4%
    M.N. Achasov, et. al., Phys.Rev.D 93 092001 (2016)
  - $e^+e^- \to K^+K^-$, agrees with BABAR, similar precision
- first experimental measurements
  - $e^+e^- \to \pi^+\pi^-\pi^0\eta$
  - $e^+e^- \to \omega\pi^0\eta$

Recent $e^+e^- \to$ hadrons results from SND at VEPP-2000 (Mikhail Achasov)

SND data

About 15 hadronic processes are currently under analysis.

VEPP-2M			
	Below φ	Arround φ	Above φ
IL, pb-1	9,1	13,2	8,8
√s, GeV	0,36 – 0,97	0,98 – 1,06	1,06 – 1,38

VEPP-2000			
	Below φ	Arround φ	Above φ
IL, pb-1	15,4	6,9	47,0
√s, GeV	0,30 – 0,97	0,98 – 1,05	1,05 – 1,38

Here we report the four results

Precision measurements

$e^+e^- \to \pi^0\gamma$ (VEPP-2M data)

$e^+e^- \to K^+K^-$

First measurements

$e^+e^- \to \pi^+\pi^-\pi^0\eta$

$e^+e^- \to \omega\pi^0\eta$

4

Recent $e^+e^- \to$ hadrons results from SND at VEPP-2000 (Mikhail Achasov)

$e^+e^- \to \pi^0\gamma$ cross section

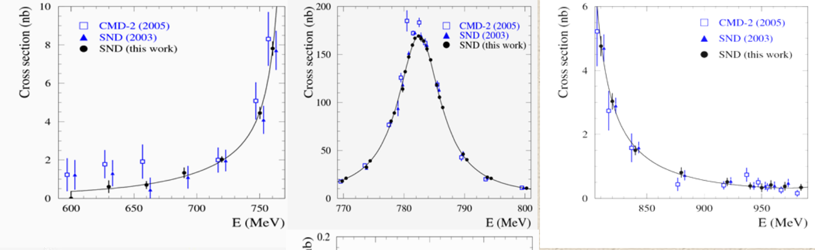

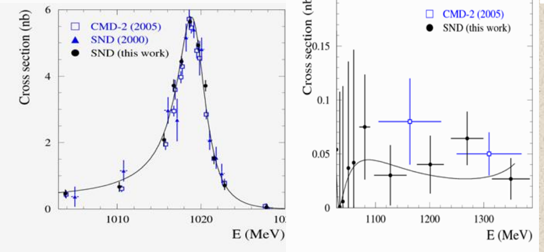

- The most precise measurement of the $e^+e^- \to \pi^0\gamma$ cross section.
- Systematic uncertainty at the ω peak is **1.4%** (**1.2%** from luminosity and **0.6%** due to selection criteria)

M.N. Achasov, et. al., Phys. Rev. D 93 092001 (2016)

7

Recent $e^+e^- \to$ hadrons results from SND at VEPP-2000 (Mikhail Achasov)

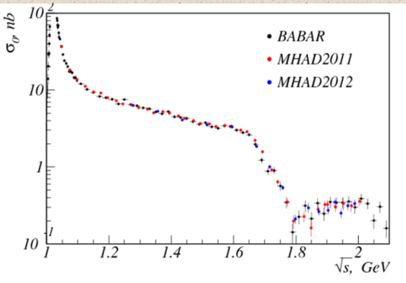

$e^+e^- \to K^+K^-$

SND measurement agrees with the BABAR data and has comparable or better accuracy.

The **green** and **yellow** bands represent the **BABAR** and **SND** systematic uncertainties.

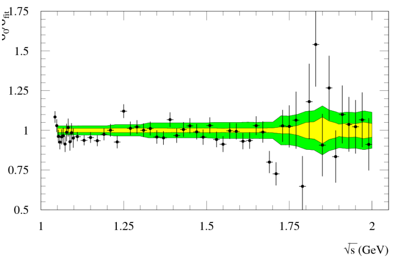

(BABAR data)/(SND fit) ratio

10

Recent $e^+e^- \to$ hadrons results from SND at VEPP-2000 (Mikhail Achasov)

$e^+e^- \to \pi^+\pi^-\pi^0\eta$

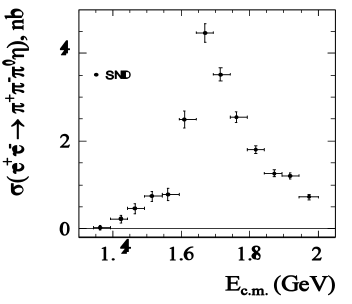

- First measurement of this process.
- Intermediate states are $\omega\eta$, $\phi\eta$, strucureless $\pi^+\pi^-\pi^0\eta$ and $a_0(980)\rho$.
- The known $\omega\eta$ and $\phi\eta$ contributions explain about 50-60% of the cross section below **1.8 GeV**.
- Above **1.8 GeV** the dominant reaction mechanism is $a_0(980)\rho$.

- The process $e^+e^- \to \omega\eta$ has been measured separately.
- There is a significant difference between **SND** result and the previous **BABAR** measurement.

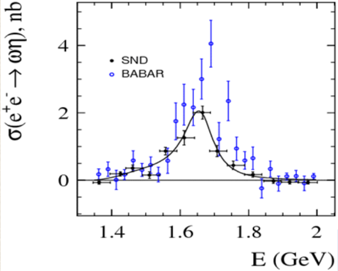

14

Recent $e^+e^- \to$ hadrons results from SND at VEPP-2000 (Mikhail Achasov)

$e^+e^- \to \omega\pi^0\eta$

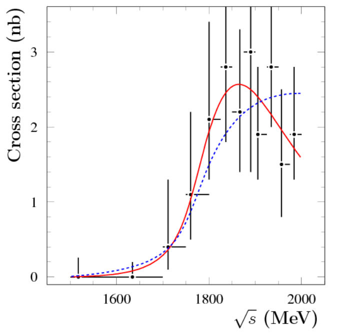

- First measurement of the $e^+e^- \to \omega\pi^0\eta$ cross section.
- The dominant reaction mechanism is $\omega a_0(980)$.
- The cross-section energy dependence is fitted by **two** models.
- **Red** line corresponds to a single-resonance model. The resonance's parameters are consistent with those for $\rho(1700)$.
- **Blue** line corresponds to $\omega a_0(980)$ phase space model.
- **Both** models are consistent with data.

The cross section is about **2.5 nb**, **5%** of the total hadronic cross section in the energy region **1.8 – 2.0 GeV**.

16

Recent $e^+e^- \to$ hadrons results from SND at VEPP-2000 (Mikhail Achasov)

Conclusions

- During **2010 – 2013** the **SND** detector accumulated **~70 pb^{-1}** of integrated luminosity at the **VEPP-2000** electron-positron collider in the c.m. energy range **0.3 – 2 GeV**.
- Data analysis on hadron production is in progress. The obtained results have comparable or better accuracy than previous measurements (**$\omega\pi^0$, $\pi^+\pi^-\pi^0$, $\pi^+\pi^-\eta$, n anti-n, $\pi^0\gamma$, K^+K^-**).
- For several processes the cross sections have been measured for the first time (**$\eta\gamma$, $\pi^+\pi^-\pi^0\eta$, $\omega\pi^0\eta$**).
- After **VEPP-2000** upgrade the data taking runs will be continued with a goal of **~1 fb^{-1}** of integrated luminosity.

17

Progress on the experimental measurements of $e^+e^- \to$ hadrons

Novosibirsk, CMD-3 at VEPP-2000 measurements

- goal to measure $e^+e^- \to \pi^+\pi^-$ at 0.3-0.5% and multi-body at $\sim$3%
- $\leq 0.3\%$ luminosity measurements
- in progress:
  - $e^+e^- \to \pi^+\pi^-$,
  - $e^+e^- \to K^+K^-$ (2.5% precision),
  - $e^+e^- \to \pi^+\pi^-\pi^0$ (current precision 7%),
  - $e^+e^- \to 2\pi^+2\pi^-$,
  - $e^+e^- \to 5\pi$,
  - $e^+e^- \to 6\pi$,
  - $e^+e^- \to 2\pi^+2\pi^-$,
  - $e^+e^- \to \eta(\gamma\gamma)\pi^+\pi^-$,
  - $e^+e^- \to K^+K^-\pi^0$,
  - $e^+e^- \to \phi\eta \to K^+K^-\eta$,
  - $e^+e^- \to K^+K^-\omega$,
  - $e^+e^- \to \omega \to \pi^0e^+e^-$,
  - $e^+e^- \to \pi^0\gamma, \eta\gamma \to 3\gamma$
- published $e^+e^- \to K^0_S K^0_L$, syst.err. 2–3% Phys.Lett. B760 (2016) 314-319
- published $e^+e^- \to K^+K^-\pi^+\pi^-$, Phys.Lett. B756 (2016)153-160

New $e^+e^- \to$ hadrons results from CMD-3 (Simon Eidelman)

$e^+e^- \to K_L K_S$

This process is studied using decay $K_s \to \pi^+\pi^-$

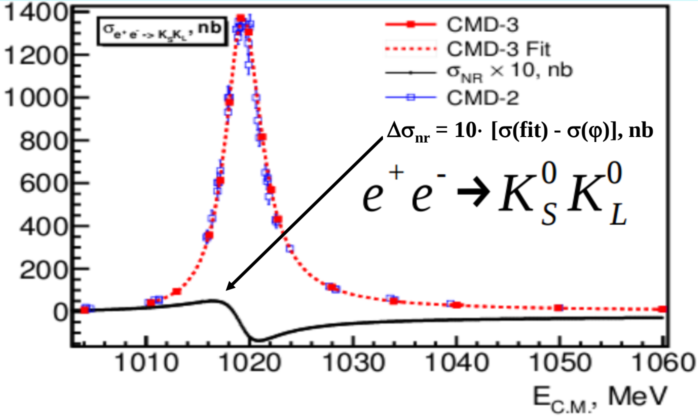

In E_{cm} = 1004 – 1060 MeV: 25 energy points. Collected luminosity ~5.9 pb^{-1}

Systematic error is 2 – 3 %

Published in **Phys.Lett. B760 (2016) 314-319**

14

New $e^+e^- \to$ hadrons results from CMD-3 (Simon Eidelman)

$e^+e^- \to K^+K^-\pi^+\pi^-$

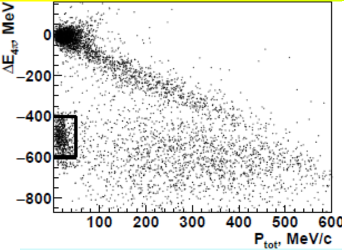

$\Delta E = E_1 + E_2 + E_3 + E_4 - 2E_{beam}$
$P_{tot} = |P_1 + P_2 + P_3 + P_4|$

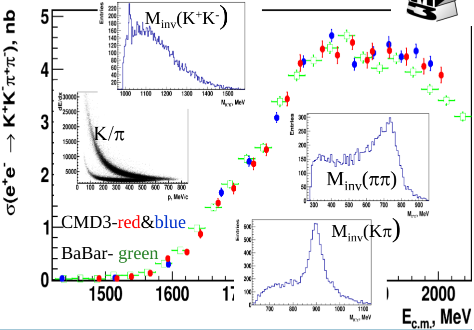

- CMD-3 studies uses 22 pb^{-1} between 1.5 and 2 GeV, more than 20000 events with 3 and 4 tracks were selected for analysis;
- Ionisation losses in DC dE/dx provide good K/π separation;
- Analysis of $\pi^+\pi^-$, $K^\pm\pi^\mp$, K^+K^- inv. Masses clear shows signals from π^0, $K^{*0}(892)$ and $\phi(1020)$;
- Many different mechanisms seen: $K_1(1270)K \to K2\pi K$, $K^*(892)K\pi$, $K_1(1400)K \to K^*(892)\pi K$, $\varphi\pi^+\pi^-$.

Recently published in Phys.Lett. B756 (2016)153-160

Progress on the experimental measurements of $e^+e^- \to$ hadrons

Novosibirsk, KEDR at VEPP-4M

- R measurements between J/ψ and $\psi(2S)$
  V.V. Anashin et al., Phys.Lett. B753, 533 (2016)
- R measurements between 1.84–3.05 GeV, systematic precision 2.1–3.7%, agrees with perturbative QCD

R measurement between 1.8 and 3.7 GeV at KEDR (Simon Eidelman)

VEPP–4M collider

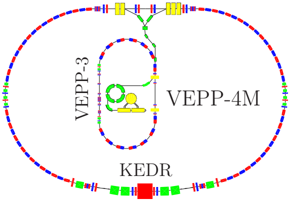

Circumference	366 m
Beam energy	$1 \div 5$ GeV
Number of bunches	2×2
Luminosity, $E = 1.5$ GeV	2×10^{30} cm^{-2}s^{-1}
Luminosity, $E = 5.0$ GeV	2×10^{31} cm^{-2}s^{-1}

- Resonant depolarization technique:
  Instantaneous measurement accuracy $\simeq 1 \times 10^{-6}$
  Energy interpolation accuracy $(5 \div 15) \times 10^{-6}$ $(10 \div 30$ keV$)$
- Infrared light Compton backscattering:
  Statistical accuracy $\simeq 5 \times 10^{-5}$ / 30 minutes
  Systematic uncertainty $\simeq 3 \times 10^{-5}$ $(50 \div 70$ keV$)$

Preliminary 2016 update of DHMZ a_μ^{th} (Michel Davier, Tau 2016)

- a_μ^{hadLO} DHMZ 2011 evaluation updated to 2016
  - (Davier-Hoecker-Malaescu-Zhang)
  - more complete data from *BABAR*, KLOE, BESIII, CMD3, SND, VEPP-2000, KEDR
  - value similar to 2011, uncertainty from 0.61% to 0.48%
  - Theory vs. experiment discrepancy now 3.6σ

Review of g-2 predictions with experimental inputs (Michel Davier)

Our group contribution to LO Hadronic a_μ^{had}

The dispersive approach follows the availability of trustful experimental data

- Use data on e+e- → hadrons and on τ → ν hadrons (CVC+isospin breaking), more precise then Alemany-Davier-Hoecker 1997
- Detailed QCD studies of τ decays (ALEPH) and tests of quark-hadron duality ⇒ substitute pQCD above 1.8 GeV to less precise data Davier-Hoecker 1998,98
- Update with new data from VEPP-2M Davier-Eidelman-Hoecker-Zhang 2003,03
- Detailed study of isospin-breaking effects when using τ spectral functions Davier-Hoecker-Lopez-Malaescu-Mo-Toledo-Wang-Yuan-Zhang 2010
- Improvement of statistical and systematic tools (HVPTools) and update with new BABAR π+π− data Davier-Hoecker-Malaescu-Yuan-Zhang 2010
- Global update Davier-Hoecker-Malaescu-Zhang 2011
- New update today, taking advantage of more complete data from BABAR, KLOE, BESIII, CMD3 and SND at VEPP-2000, KEDR

Tau2016 Beijing Sept. 19-23 Michel Davier (davier@lal.in2p3.fr, LAL, Orsay) 5

Review of g-2 predictions with experimental inputs (Michel Davier)

Input e+e- Data in Combination with pQCD

Davier-Hoecker-Zhang, RMP 78 (2006) 1043

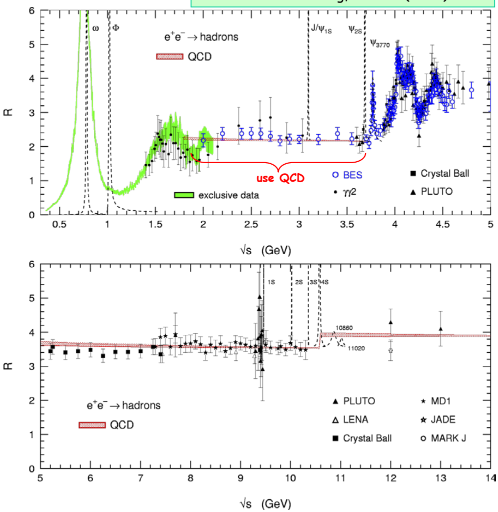

- $[\pi^0\gamma$-1.8GeV]
  - sum about 22→37 exclusive channels
  - estimate unmeasured channels using isospin relations
- [1.8-3.7] GeV
  - good agreement between data and pQCD calculation; previous extensive QCD tests with τ data
    → use 4-loop pQCD
  - J/ψ, ψ(2s): Breit-Wigner integrals
- [3.7-5] GeV
  charm particle thresholds
  → use data
- >5GeV
  use 4-loop pQCD calculation

Tau2016 Beijing Sept. 19-23 6

Review of g-2 predictions with experimental inputs (Michel Davier)

a_μ Tau 2016 preliminary

$a_\mu^{had\ LO}$

DEHZ 2003 $696.3 \pm 6.2_{exp} \pm 3.6_{rad}$ (7.1_{tot})

DHMZ 2011 $692.3 \pm 1.4_{stat} \pm 3.1_{syst} \pm 2.4_{corrsyst} \pm 0.2_{\psi} \pm 0.3_{QCD}$ (4.2_{tot})

DHMZ 2016 $692.8 \pm 1.2_{stat} \pm 2.6_{syst} \pm 1.6_{corrsyst} \pm 0.1_{\psi} \pm 0.3_{QCD}$ (3.3_{tot})

a_μ

QED	11658471.885	+- 0.004
EW	15.4	+- 0.1
had LBL	10.5	+- 2.6
had LO	692.8	+- 3.3
had NLO	-9.87	+- 0.09
had NNLO	1.24	+- 0.01
prediction	11659181.9	+- 4.2
exp BNL	11659208.9	+- 6.3

deviation	27.0	+- 7.6	3.6σ

Tau2016 Beijing Sept. 19-23 Michel Davier (davier@lal.in2p3.fr, LAL, Orsay) 23

Review of g-2 predictions with experimental inputs (Michel Davier)

R(s) 2016

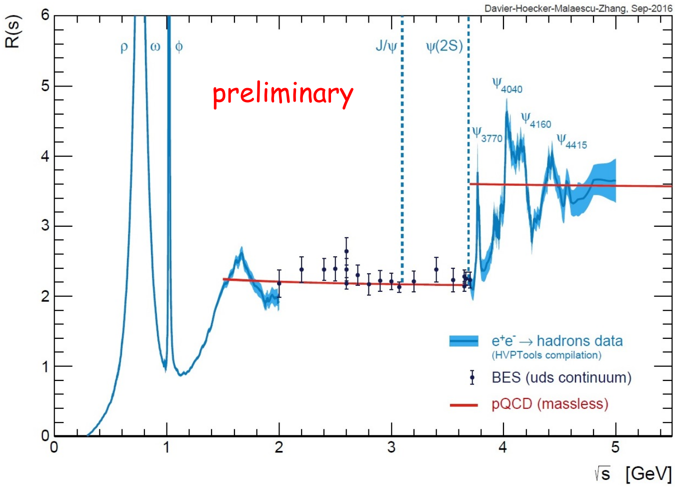

Tau2016 Beijing Sept. 19-23 Michel Davier (davier@lal.in2p3.fr, LAL, Orsay) 25

Conclusions

- one single experiment, BNL E821, dominates measurement of a_μ^{exp} (540 ppb)
- two next generation experiments are in preparation
  - FNAL E989, begins data-taking in 2017, goal 140 ppb
  - J-PARK E34, revised TDR in 2016, goal 1st phase 370 ppb
- steady progress on exp. measurements for a_μ^{hadLO}
  - $\delta a_\mu^{\text{hadLO}}$ from 420 ppb (2011) to 360 ppb (Davier *et al.*, 2016)
  - conceivable to reduce $\delta a_\mu^{\text{hadLO}}$ to 210 ppb during E989 measurement